Received: 5 August 2022 | Revised: 20 February 2023 | Accepted: 9 March 2023

DOI: 10.1002/mp.16393

TECHNICAL NOTE

MEDICAL PHYSICS

Technical note: Angular dependence in fiber optic dosimetry using $YVO_4:Eu^{3+}$

Nahuel Martínez[1,2] | **Yohanna Fernández**[1] | **Soledad Machello**[3] | **Pablo Molina**[1] | **José Massa**[4] | **Martín Santiago**[1]

[1]CIFICEN (UNCPBA-CICPBA-CONICET), Tandil, Argentina

[2]LBN (UNQ-CONICET), Bernal, Argentina

[3]CIO, Tandil, Argentina

[4]INTIA (FCEx-UNCPBA), Tandil, Argentina

Correspondence
Nahuel Martínez, CIFICEN (UNCPBA-CICPBA-CONICET), Pinto 399, (7000) Tandil, Argentina.
Email: nahuelm@ifas.exa.unicen.edu.ar

Funding information
ANPCyT, Grant/Award Number: PICT 2015-1555; CONICET, Grant/Award Number: PIP 0800-2015-2017

Abstract

Background: Fiber optic dosimetry (FOD) has emerged as a useful technique that can be used in those cases when intracavitary, real time, high spatial resolution dose assessment is required. Among the several factors characterizing a dosimeter, angular response of FOD probes has to be assessed in order to consider possible clinical application.

Purpose: The objective of this study was to characterize the angular response of a FOD probe based on a cylindrical shaped $YVO_4:Eu^{3+}$ scintillator under irradiation with a 6 MV photon beam generated by a linear accelerator (LINAC).

Methods: A FOD probe was irradiated inside a plastic phantom using a 6 MV LINAC photon beam at different azimuthal angles (0° to 360°, 15° steps). Scintillation output was measured with a photomultiplier tube. Similar measurements were performed with a second FOD probe having an optical filter interposed between the scintillator and the fiber. Monte Carlo simulations using PENELOPE were carried out in order to interpret the observed results.

Results: The FOD output was symmetrical with respect to the scintillator axis. For the unfiltered probe, the signal was maximum at rear incidence (0°) and steadily decreased down to its minimum value at frontal incidence (180°) having a signal ratio of 37%. The output of the filtered probe showed a plateau from 15° up to 115°. The signal was maximum at 60° and minimum at 180° having a signal ratio of 16%. Monte Carlo simulations predicted symmetry of the deposited dose about 0° and 90°, which contrasts with experimental findings.

Conclusions: Photoluminescence (PL) of the scintillator induced by the Cherenkov light increases the angular dependence. Radiation attenuation inside the scintillator and partial light collection of the scintillation yield by the optical fiber (OF) are responsible for asymmetrical response. Results from this study should be considered in order to minimize angular dependence in FOD.

KEYWORDS
angular dependence, Eu3+, fiber optic dosimetry

1 | INTRODUCTION

In recent years radiotherapy techniques have increased their complexity requiring the development of new dosimetry systems. In particular, treatments involving high doses and steeply varying dose gradients call for high spatial resolution and real-time dose assessment systems.[1–3] Fiber optic dosimetry (FOD) has the potential to meet this need.[4–7]

Both organic and inorganic compounds have been investigated as luminescent detectors in FOD, with plastic scintillators (PSs) the most studied materials so far.[7] PSs are made of aromatic hydrocarbon molecules, thus absorbing ionizing radiation similarly to water and soft tissue at megavoltage photon energies.[8] For this reason, PSs are considered tissue equivalent ionizing radiation detectors, which is one of their most relevant characteristics. One drawback affecting PSs is their

relatively low scintillation light yield, which poses a challenge to optimize optical coupling and light collection in PS-based FOD instrumentation.[9]

Inorganic scintillators (ISs) have also attracted attention as detectors in FOD.[10] ISs are mainly alkali halide or oxide crystals, usually doped with different activators.[11] Since most ISs are high-Z materials, they show an overresponse to low-energy photons (less than 100 keV). For this reason, the application of ISs in FOD has received less attention than PSs to date.[10] Despite this drawback, ISs feature scintillation yields that are at least one order of magnitude greater than PSs.[12,13]

The response of a dosimeter may depend on several factors (temperature, source to detector distance, dose rate, accumulated dose, etc.).[14] In particular, the dependence of the dosimeter response on the relative orientation of detector and source (angular response) is a feature that must be known before clinical use of the dosimetric system.[15] In the case of FOD, the key point is to determine the dependence of the response on the angle between the radiation beam and the scintillator axis in the azimuthal plane, since the response of most FOD probes features axial symmetry.[16]

The main drawback affecting FOD is the stem effect, a combination of fluorescence and Cherenkov radiation produced in the exposed portion of the optical fiber (OF). The stem effect adds to the radioluminescence (RL) signal, producing a bias in the dose rate measurement. Several methods have been put forward to reduce the stem effect, which are useful in different situations.[17] The time-gated technique is suitable for filtering the short-lived Cherenkov signal in LINACs when the scintillator features a long decay time of its RL signal of the order of 1 ms.[18] Practical applications of the time-gated method in high-Z_{eff} ISs have been reported in $YVO_4:Eu^{3+}$ (Z_{eff} = 25,4) and Gd_2O_2S:Tb-based FOD systems.[19–21]

The ultraviolet component of the Cherenkov radiation may induce photoluminescence (PL) in the scintillator, which also adds to the RL signal. Cherenkov-induced PL could be decreased using a plastic long-pass filter between scintillator and the OF.[12]

The intensity of the Cherenkov light produced in an OF depends on the angle between the radiation beam and the fiber axis.[22] In the case of electron beams, the intensity of the Cherenkov radiation is minimized when the fiber is orthogonal to the beam axis.[23] When an OF is irradiated with photons, the angular dependence of the Cherenkov radiation transmitted along the fiber is less pronounced, since electrons crossing the OF are secondary radiation not moving strictly in the direction of the photon beam.[24]

In this work, we studied the angular dependence of the RL signal from a $YVO_4:Eu^{3+}$-based FOD probe irradiated with 6 MV photons from a clinical LINAC. Monte Carlo simulations were carried out and compared to the experimental results. The effect of adding an optical filter between the IS and the OF in order to reduce the contribution of the Cherenkov-induced PL signal to the angular response of the FOD probe was also investigated.

2 | MATERIALS AND METHODS

2.1 | FOD probe design and experimental setup

The probes employed in this work were made with $YVO_4:Eu^{3+}$ powder (Phosphor Technologies, UK) as scintillator material. $YVO_4:Eu^{3+}$ shows strong luminescence at 620 nm when excited with ionizing radiation.[12] Two FOD probes were prepared. One of them (probe A) consisted of a cylindrical detector (1 mm diameter, 2 mm length) directly attached to the end of a PMMA SuperEska OF (10 m length, 1 mm diameter). The other one (probe B) was identical to probe A except that an optical filter was placed between the OF and the scintillator powder. The optical filter prevented the UV component of the Cherenkov radiation produced in the OF from exciting PL from the scintillator. A tiny piece of gel filter (Roscolux 027) was employed for this purpose. The OFs were terminated with SMA connectors. Further details of the probe fabrication were described in previous work.[20]

The intensity of the scintillation light from the FOD probes was measured by means of a Hamamatsu H9319-02 photon counting head placed outside the irradiation room and connected to a data acquisition device (National Instruments USB-6251 DAQ).

The 6 MV photon beam of a Varian LINAC was employed to irradiate the FOD probes. The contribution of the stem effect was reduced by resorting to the time-gated method, as described in previous work.[19] The time-gated filter was set to measure the light signal 20 μs after the beginning of each LINAC pulse.

2.2 | Measurements

2.2.1 | Angular response of the FOD probe

The angular response of probes A and B was recorded at different angles between the probe axis and the photon beam (azimuthal plane). The tip of the FOD probe was inserted upwards through a hole in the center of a lab-made PMMA phantom (see Figure 1) and positioned at the LINAC isocenter (at 100 cm from the x-ray source). The angular response of the probe was measured from 0° to 360° at intervals of 15°. $\theta = 0°$ corresponds to the beam entering through the fiber before encountering the scintillator (rear incidence). $\theta = 180°$ corresponds to frontal incidence. The angle was varied by rotating the LINAC gantry. A 50 monitor units (MU) irradiation was delivered to the FOD probe at each angle. An irradiation field of 2×2 cm^2 at the

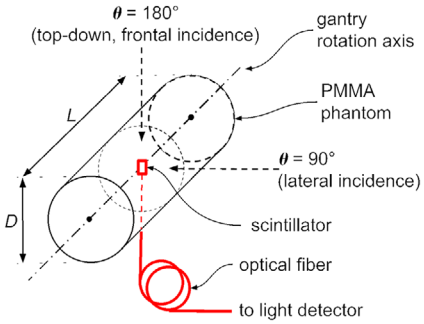

FIGURE 1 The experimental setup employed to measure the response dependence on the azimuthal angle. The dimensions of the cylindrical phantom were $L = 5$ cm and $D = 3$ cm.

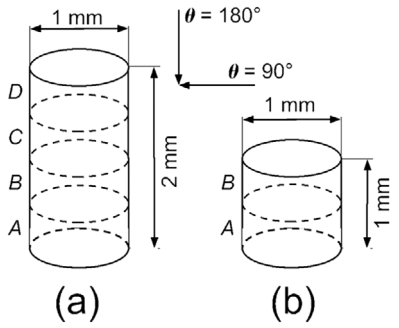

FIGURE 2 Geometry of the detector considered for Monte Carlo simulations. Each cylindrical scintillator is made up of four (a) or two (b) 0.5 mm length disks. The scintillators were inside a cylindrical phantom emulating the measurements. Normal (90°) and top-down (180°) incidence angles are indicated.

isocenter was employed. In this work, only the response at different angles in the azimuthal plane was measured, since angular response symmetry in the radial plane has already been established.[20]

2.3 | Monte Carlo simulations

The experimental setup described in Section 2.2.1 was modeled by Monte Carlo simulations. In particular, the dose delivered to the FOD probe at different azimuthal angles was estimated by means of the PENELOPE Monte Carlo code. The 2×2 cm^2 square field was simulated using the SPYRAM function.[25] The source was placed on the irradiation Z-axis, 100 cm above the origin. The 6 MV photon beam was simulated with the following energy spectrum as described in a previous work: 5 MeV (6.59%), 3 MeV (25.04%), and 1 MeV (68.37%).[26] The simulation parameters for absorption energy, elastic scattering and cut-off energy were set to (1e5, 1e4, 1e5), (0.1, 0.1), and (1e3; 1e4) eV respectively. The angle between the photon beam and the scintillator axis was varied between 0° and 180° at 15° steps. The number of simulated showers was 10^9 at every angular position for each probe considered.

2.3.1 | Simulation geometry

The cylindrical scintillator was simulated with a stack of four disks of 0.5 mm length and 1 mm diameter (see Figure 2a). The disks were identified as A, B, C, and D. The energy in eV deposited in each disk was calculated. The total energy deposited in the scintillator was taken to be the simple sum of the energy deposited in each disk. In order to investigate the dependence of the dose on the detector size a shorter scintillator was also modeled having a 1 mm length. In this case, the detector was made up of two disks, namely, A and B (see Figure 2b). In both cases, the detector was placed inside a PMMA cylindrical phantom of 50 mm length and 30 mm diameter, identical to the phantom employed for the measurements. The OF was not simulated, since it is made of the same material as the phantom. For the simulations the relative orientation of detector, phantom and beam was identical to that shown in Figure 1.

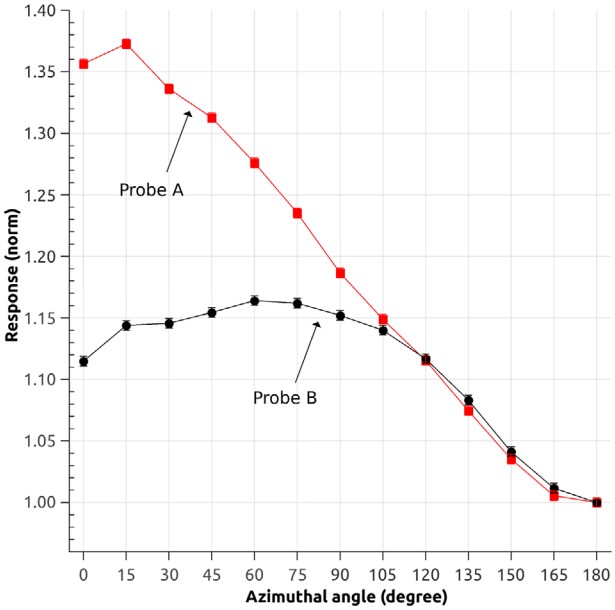

FIGURE 3 Response of YVO_4:Eu^{3+}-based FOD probes A and B corresponding to different incidence angles between 0° (bottom-up incidence) and 180° (top-down incidence). The time-gated filter was applied in both cases in order to reduce the contribution of the stem effect. Values were normalized to the signal measured at 180°.

3 | RESULTS AND DISCUSSIONS

3.1 | Angular response of the FOD probe

The intensity of the RL signal corresponding to both probes A and B as function of the azimuthal angle between the photon beam and the OF axis is shown in Figure 3. Both signals were time-gated filtered, which

means that the Cherenkov component of the stem effect is not present. As expected the RL signal was symmetric with respect to 180° (top-down incidence). For this reason only the response from 0° to 180° is shown. The measured values were normalized to the signal measured at $\theta = 180°$ (frontal incidence), which is the angle where the minimum signal is observed for both probes. Error bars correspond to the standard deviation of the signal recorded by the photon counting head during the 50 MU irradiation. Measured differences between maximum and minimum are 37% and 16% for probes A and B respectively. Figure 3 shows that the response is not symmetric around 90° (normal incidence), as would be expected considering the cylindrical shape of the detector. In fact, the RL signal is particularly higher when the probe is irradiated at lower angles. Comparison of the two curves shows that suppressing the Cherenkov-induced PL component by means of the optical filter has a dramatic effect on the measured signal, especially at incidence angles below 90°. The difference between the two curves observed at angles below 90° implies that the Cherenkov induced PL is an important component of spurious light in $YVO_4:Eu^{3+}$-based FOD.

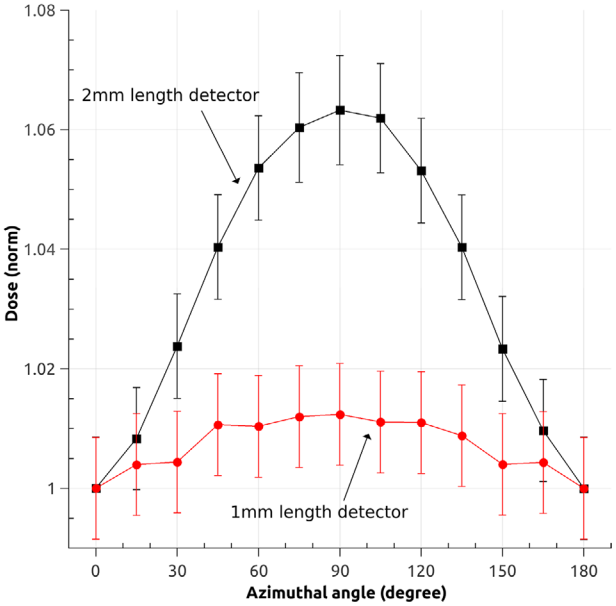

FIGURE 4 Dose deposited in $YVO_4:Eu^{3+}$ cylinders having 2 and 1 mm length calculated for different incidence angles by means of Monte Carlo simulations. All values were normalized to the dose obtained at 180°. Connecting lines have been included for the sake of clarity.

3.2 | Monte Carlo simulations

3.2.1 | Angular dependence of dose

The results of the Monte Carlo calculations of the dose deposited in $YVO_4:Eu^{3+}$ cylinders having 2 and 1 mm length are shown in Figure 4 as black squares and red circles respectively. Error bars correspond to the statistical uncertainty reported by Penelope for each simulation.

In both cylinders, the dose as function of the incidence angle is symmetric to both 0° (axial incidence) and 90° (normal incidence), as expected. In both cases (1 and 2 mm length) the dose is maximum at normal incidence (90°). This effect is more pronounced in the case of the 2 mm length detector. The maximum response at normal incidence is attributed to the maximum cross section of the detector being exposed to the beam. The relative difference between the dose calculated at 90° and 0° incidence is 6.5% and 1% for the 2 and 1 mm length cylinders respectively. Smaller variations of the angular response are expected if lower Z_{eff} scintillators are employed. In fact, Monte Carlo simulations of the angular response of a BCF-400 (polyvinyltoluene) cylinder (1 mm diameter, 4 mm length) exposed to 6 MV photons showed a relative response variation of at most 0.8%.[27] These results suggest that the overall symmetry of the detector could affect the angular response of FOD systems when $YVO_4:Eu^{3+}$ scintillators are employed and this situation should therefore be taken into account when designing the FOD probe.

The measured angular response of probe B (Figure 3, black circles) and the dose calculated by Monte Carlo at different angles (Figure 4, black squares) present differences. The experimental angular response is not symmetrical with respect to normal incidence. In fact, at incidence angles lower than 90° the signal from probe B barely decreases with respect to that measured at normal incidence. Similar results were found with FOD probes that employ other high-Z materials as scintillators. In fact, in a Gd_2O_2S:Tb-based probe the signal yielded by the scintillator was found to be maximum when the probe is irradiated at incidence angles of −45° and 45° (in our coordinate system).[16]

In order to get a better understanding of the contrast observed between the angular response of probe B (Figure 3) and the doses calculated by Monte Carlo at different angles (Figure 4), the doses calculated for each of the four disks making up the 2 mm length cylinder are plotted as a function of the incidence angle in Figure 5. As expected, the results corresponding to disks A and B are mainly specular of D and C with respect to the normal incidence (90°) respectively. Figure 5 demonstrates that in spite of the tiny dimensions of the dosimeter, the disk closest to the radiation source receives almost 20% more dose than the farthest one. This effect can be attributed to several factors. Among them, the attenuation of the beam when crossing the scintillator and the lack of charge particle equilibrium due to the small size of the radiation field could be the most important. We assume that the light yield produced at each single volume of the scintillator is proportional to the absorbed

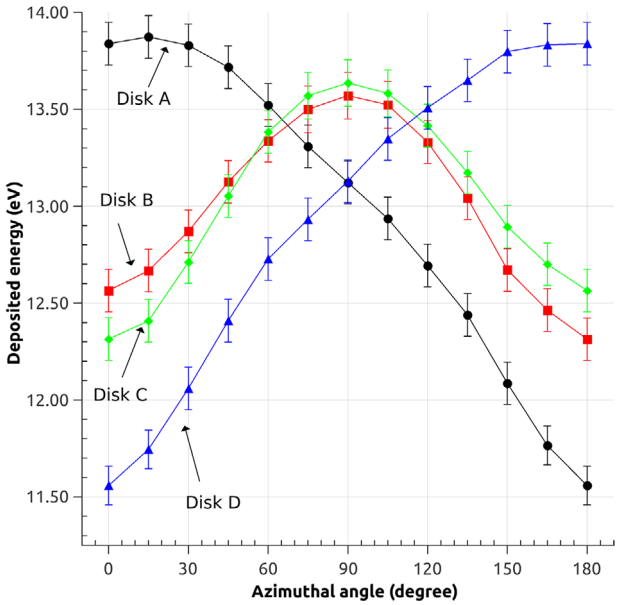

FIGURE 5 Dose absorbed by each of the four disks making up the $YVO_4:Eu^{3+}$ cylinder that simulates the 2 mm length detector.

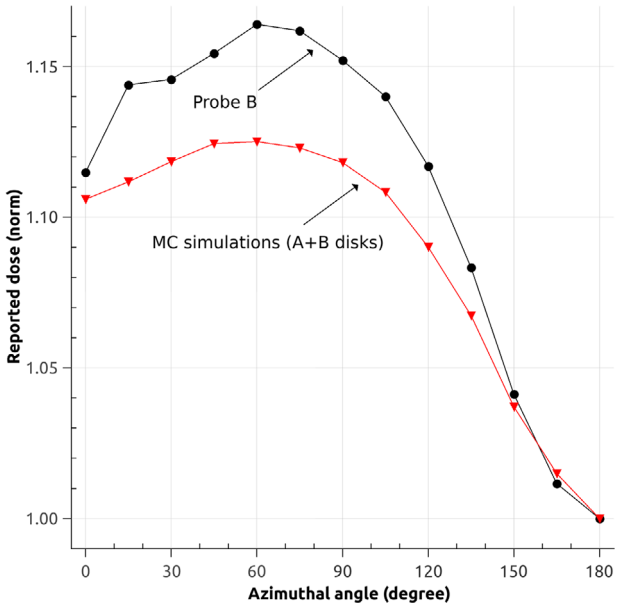

FIGURE 6 Angular response of probe B and the sum of the doses corresponding to disks A and B, as calculated by Monte Carlo simulations. Results are normalized to the response at 180°.

dose at that point. However, scintillation photons produced near the fiber end have a higher chance of being collected than those produced in the distal powder layers. In fact, the light collection efficiency depends, among several factors, on the average particle size and powder packing density.[28] Following this reasoning, in Figure 6 the angular response of probe B is compared to the sum of the doses calculated for disks A and B (after normalization at 180°). This figure shows that the main trend of the experimental curve can be recovered from the Monte Carlo simulation if we make the rough assumption that only the scintillation light produced in disks A and B is collected by the OF. In this context, the lack of symmetry of the angular response of probe B with respect to normal incidence and the over-response at low-angle incidence could be the result of both differential dose deposition throughout the detector (self-shielding) and partial collection of the scintillation light. These rather qualitative results show the importance of transparency, shape, and size of the detector when high-Z_{eff} ISs are used in FOD.

4 | CONCLUSIONS

The angular dependence of $YVO_4:Eu^{3+}$ powder based FOD probes was simulated and compared to experimental results when the probes are irradiated with 6 MV photons at a LINAC.

The time-gated technique was employed to reduce the contribution of the Cherenkov light produced in the fiber by the ionizing radiation to the signal recorded by the photodetector. The Cherenkov light induced PL in the scintillator. The intensity of the PL depends on the angle between the beam and the detector axis. Its spurious contribution was successfully minimized by placing an optical filter between the scintillator and the OF. The signal recorded by the photodetector was minimum at $\theta = 180°$ and maximum at $\theta = 60°$.

Monte Carlo simulations suggest that a self-shielding effect combined with partial collection of the scintillation light may be responsible for the angular dependence observed in this probe. This implies that the shape and size of the active volume play a significant role in the angular dependence of a FOD probe when $YVO_4:Eu^{3+}$ is used as scintillator, even for small volumes (<1 mm^3). As a rule of thumb, detectors not longer than 1 mm should be employed to reduce the angular dependence of this detector's response.

ACKNOWLEDGMENTS

The authors would like to acknowledge the financial support received from PICT 2015-1555 (ANPCyT, Argentina) and PIP 0800-2015-2017 (CONICET, Argentina).

CONFLICT OF INTEREST STATEMENT

There is no ethical problem or conflicts of interest to declare.

REFERENCES

1. International Atomic Energy Agency. *Dosimetry of Small Static Fields Used in External Beam Radiotherapy an International Code of Practice for Reference and Relative Dose Determination. IAEA and AAPM*; 2017. http://inis.iaea.org/search/search.aspx?orig_q=RN:49069982

2. Dwivedi S, Kansal S, Dangwal VK, Bharati A, Shukla J. Dosimetry of a 6 MV flattening filter-free small photon beam using various detectors. *Biomed Phys Eng Express*. 2021;7(4):045004. doi:10.1088/2057-1976/abfd80
3. Pettinato S, Girolami M, Olivieri R, Stravato A, Caruso C, Salvatori S. Time-resolved dosimetry of pulsed photon beams for radiotherapy based on diamond detector. *IEEE Sens J*. 2022;22(12):12348-12356. doi:10.1109/JSEN.2022.3173892
4. Beddar AS, Mackie TR, Attix FH. Water-equivalent plastic scintillation detectors for high-energy beam dosimetry: I. Physical characteristics and theoretical considerations. *Phys Med Biol*. 1992;37(10):1883-1900. doi:10.1088/0031-9155/37/10/006
5. Andersen CE, Rosenfeld A, Kron T, D'Errico F, Moscovitch M. Fiber-coupled luminescence dosimetry in therapeutic and diagnostic radiology. *AIP Conf Proc*. 2011;100:100-119. doi:10.1063/1.3576161
6. O'Keeffe S, McCarthy D, Woulfe P, et al. A review of recent advances in optical fibre sensors for in vivo dosimetry during radiotherapy. *Br J Radiol*. 2015;88(1050):20140702. doi:10.1259/bjr.20140702
7. Beddar S, Tendler I, Therriault-Proulx F, Archambault L, Beaulieu L. Recent advances and clinical applications of plastic scintillators in the field of radiation therapy. In: Hamel M, ed. *Plastic Scintillators: Chemistry and Applications. Topics in Applied Physics*. Springer International Publishing; 2021:425-460. doi:10.1007/978-3-030-73488-6_12
8. Hupman MA, Hill IG, Syme A. Measuring small field profiles and output factors with a stemless plastic scintillator array. *Med Phys*. 2022;49(1):624-631. doi:10.1002/mp.15357
9. Beaulieu L, Beddar S. Review of plastic and liquid scintillation dosimetry for photon, electron, and proton therapy. *Phys Med Biol*. 2016;61(20):R305-R343. doi:10.1088/0031-9155/61/20/R305
10. Ding L, Wu Q, Wang Q, Li Y, Perks RM, Zhao L. Advances on inorganic scintillator-based optic fiber dosimeters. *EJNMMI Phys*. 2020;7(1):60. doi:10.1186/s40658-020-00327-6
11. Kumar V, Luo Z. A review on x-ray excited emission decay dynamics in inorganic scintillator materials. *Photonics*. 2021;8(3):71. doi:10.3390/photonics8030071
12. Kertzscher G, Beddar S. Inorganic scintillation detectors based on Eu-activated phosphors for192Ir brachytherapy. *Phys Med Biol*. 2017;62(12):5046-5075. doi:10.1088/1361-6560/aa716e
13. Shaharuddin S, Hart A, Bazalova-Carter M, et al. Evaluation of scintillation detectors for ultrahigh dose-rate x-ray beam dosimetry. *Optical Sensing and Detection VII Vol 12139 SPIE*. 2022:170-177. doi:10.1117/12.2621591
14. Ruiz-Arrebola S, Fabregat-Borrás R, Rodríguez E, et al. Characterization of microMOSFET detectors for in vivo dosimetry in high-dose-rate brachytherapy with 192Ir. *Med Phys*. 2020;47(5):2242-2253. doi:10.1002/mp.14080
15. Palmans H, Andreo P, Huq MS, Seuntjens J, Christaki KE, Meghzifene A. Dosimetry of small static fields used in external photon beam radiotherapy: summary of TRS-483, the IAEA–AAPM international Code of Practice for reference and relative dose determination. *Med Phys*. 2018;45(11):e1123-e1145. doi:10.1002/mp.13208
16. Zhuang Q, Yaosheng H, Yu M, et al. Embedded structure fiber-optic radiation dosimeter for radiotherapy applications. *Opt Express, OE*. 2016;24(5):5172-5185. doi:10.1364/OE.24.005172
17. Archer J, Madden L, Li E, Wilkinson D, Rosenfeld AB. An algorithmic approach to single-probe Cherenkov removal in pulsed x-ray beams. *Med Phys*. 2019;46(4):1833-1839. doi:10.1002/mp.13383
18. Clift MA, Johnston PN, Webb DV. A temporal method of avoiding the Cerenkov radiation generated in organic scintillator dosimeters by pulsed mega-voltage electron and photon beams. *Phys Med Biol*. 2002;47(8):1421-1433. doi:10.1088/0031-9155/47/8/313
19. Martinez N, Teichmann T, Molina P, et al. Scintillation properties of the YVO4:Eu^{3+} compound in powder form: its application to dosimetry in radiation fields produced by pulsed mega-voltage photon beams. *Zeitschrift für Medizinische Physik*. 2015;25(4):368-374. doi:10.1016/j.zemedi.2015.04.001
20. Martinez N, Rucci A, Marcazzó J, Molina P, Santiago M, Cravero W. Characterization of YVO4:Eu^{3+} scintillator as detector for fiber optic dosimetry. *Radiat Meas*. 2017;106:650-656. doi:10.1016/j.radmeas.2017.03.015
21. Alharbi M, Martinez N, Foley M, Dosimetric performance of an inorganic optical fibre dosimeter when temporally separating Cherenkov radiation. In: Optical Sensing and Detection VII. Vol 12139. SPIE. 2022:185-193. doi:10.1117/12.2619329
22. Jelley JV. Cerenkov radiation and its applications. *Br J Appl Phys*. 1955;6(7):227-232. doi:10.1088/0508-3443/6/7/301
23. Beddar AS, Mackie TR, Attix FH. Cerenkov light generated in optical fibres and other light pipes irradiated by electron beams. *Phys Med Biol*. 1992;37(4):925-935. doi:10.1088/0031-9155/37/4/007
24. Jang KW, Yagi T, Pyeon CH, et al. Application of Cerenkov radiation generated in plastic optical fibers for therapeutic photon beam dosimetry. *JBO*. 2013;18(2):027001. doi:10.1117/1.JBO.18.2.027001
25. Salvat F, Fernández-Varea JM, Sempau J, et al. PENELOPE-2008: a code system for Monte Carlo simulation of electron and photon transport. In: Workshop Proceedings, Barcelona, Spain. 30. Nuclear Energy Agency, Organization for Economic Co-operation and …; 2008.
26. Rucci A, Carletti C, Cravero W, Strbac B. Use of IAEA's phase-space files for virtual source model implementation: extension to large fields. *Physica Medica*. 2016;32(8):1030-1033. doi:10.1016/j.ejmp.2016.07.006
27. Wang LLW, Klein D, Beddar AS. Monte Carlo study of the energy and angular dependence of the response of plastic scintillation detectors in photon beams. *Med Phys*. 2010;37(10):5279-5286. doi:10.1118/1.3488904
28. Liaparinos P, Kalyvas N, Katsiotis E, Kandarakis I. Investigating the particle packing of powder phosphors for imaging instrumentation technology: an examination of Gd2O2S:Tb phosphor. *J Inst*. 2016;11(10):P10001-P10001. doi:10.1088/1748-0221/11/10/P10001

How to cite this article: Martínez N, Fernández Y, Machello S, Molina P, Massa J, Santiago M. Technical note: Angular dependence in fiber optic dosimetry using $YVO_4:Eu^{3+}$. *Med. Phys*. 2023;1-6. https://doi.org/10.1002/mp.16393